# Supporting Information

Ikegami et al. 10.1073/pnas.1002128107

## SI Materials and Methods

**Animals.** To disrupt the TTLL1 gene, we replaced exons 2–4 with a TKneo cassette (derived from pMC1-Neo polyA vector; Stratagene) by homologous recombination in ES cells (129/Sv/Ev background). Genotyping of mice was performed by PCR with the following primers: 5′-TGACGTTCCCGAGTGTAAGGA-3′, 5′-GGTGAATACACTGTCACCGTC-3′, and 5′-GGTGG-AAAATGGCCGCGGGGC-3′. All analyses used littermates derived from mating heterozygous mice on a hybrid 129Sv/C57BL6 background, the backcross generations of which range from N3 to N7. The conditional *Dnaic1*-KO animal was described previously (1). All animals were treated according to guidelines approved by the Animal Care and Use Committees of the respective institutions.

**Antibodies.** Anti-TTLL1 polyclonal antibody was raised in guinea pigs immunized with purified recombinant TTLL1 fused to GST. The recombinant protein was expressed in an *Escherichia coli* strain BL21 (DE3) (Stratagene) and purified with glutathione Sepharose beads (GE Healthcare). Anti-polyglutamylated tubulin monoclonal antibody, GT335 (2) was a gift from Dr. Carsten Janke (Institut Curie). Monoclonal antibodies against α-tubulin (DM1A), acetylated tubulin (6-11B-1), and tyrosinated tubulin (1A2) and polyclonal antibodies against actin and γ-tubulin were purchased from Sigma-Aldrich. Polyclonal antibody for β-tubulin was obtained from Lab Vision. Monoclonal antibody for GAPDH (6C5) and polyclonal antibodies for detyrosinated tubulin and Δ2-tubulin were purchased from Chemicon International. Anti-Tektin2 mouse polyclonal antibody was obtained from Abnova. Alexa fluorophore-conjugated secondary antibodies were purchased from Invitrogen. HRP-conjugated secondary antibodies for Western blot analysis were obtained from Jackson ImmunoResearch Laboratories.

**Analysis of Ciliary Axoneme Bend Angle.** For analyzing the bend angle directly after isolation, resuspended ciliary axonemes were seeded on MAS-coated glass slide and fixed with 4% paraformaldehyde (PFA). When axonemes were relaxed, isolated axoneme pellets were suspended in cilia-reactivating solution as described previously (3). The relaxation of axonemes was carried out by incubating the axonemes with 2 μM ATP at room temperature (22–25 °C) for 15 min. The relaxed axonemes were fixed with 0.1% glutaraldehyde (GA) as described previously (4). This lower GA concentration was adopted to avoid axonemal distortion from a higher GA concentration (5). The effectiveness of this lower GA concentration was verified by observing its effect on stopping ciliary motility. The majority of axonemes examined demonstrated a clear curve; a few axonemes appeared damaged or had a small curvature in only a small part of the entire axoneme (Fig S4). Whereas obviously damaged axonemes were excluded from this assay, axonemes with small areas of curvature were analyzed. Axonemal lengths and areas between the arc and the chord were measured by tracing the whole length of individual axonemes using AquaCosmos image-analyzing software (Hamamatusu Photonics). Given the two measured values, bend angles were calculated as shown in Fig S4. The representative axonemal shape in Fig. 2*G* was depicted as a simple arc with the median axoneme length and the median bend angle using commercial software (Adobe Illustrator; Adobe Systems).

**Manipulation of Ciliary Beating.** Ciliated cortices were prepared from murine trachea as described previously (6) with some modifications. CHAPS was used as the membrane-removing detergent instead of Triton X-100. Relaxation and reactivation of ciliary axonemes were carried out according to published procedures (6). A microperfusion system using coverslips and cotton paper was used to replace solutions as described previously (6). Ciliary motility was recorded with a CCD camera (C4742-95; Hamamatsu Photonics) at 54 fps. Recording was done at 24–26 °C.

**Analysis of Ciliary Motility.** For analysis of isolated axonemes, an aliquot of axonemes suspended in reactivation buffer was placed in a chamber formed between two pieces of cover glass. To analyze intact cilia, tracheal tissue was transiently cultured in DMEM with 10% FBS. Cilia tips were labeled with Indian ink diluted with culture medium at 1:100. Ciliary motility was recorded with a high-speed CCD camera (C9100-02 or C9300-201; Hamamatsu Photonics) at 127 fps. Recording was done at 24–26 °C. Four independent animals for each genotype were examined. Fast Fourier transformation was done with Origin (Origin Lab). Data are given as mean ± SEM ($n$ = 40 for ink-labeled cilia of both genotypes; $n$ = 56 for isolated axonemes of WT; $n$ = 65 for those of KO). Ciliary beating frequencies were determined by subjecting original traces to fast Fourier transformation using Origin. Statistical analyses were performed by one-way ANOVA.

**Electron Microscopy.** For observation of central doublets and central sheath, tracheas were fixed with 2% GA/2% PFA. For observation of dynein arms, isolated cilia axonemes were fixed with 2% GA and 0.1% tannic acid. Scanning electron microscopy was performed after dehydration and coating of the fixed tissues with Pt and Pd. For TEM, the fixed tissues were embedded in epon resin after dehydration. Uranium-lead–stained ultra-thin sections (~50 nm) were observed under a JEM-1230 electron microscope (JEOL). The central sheath was observed after averaging 32 independent photomicrographs using Photoshop (Adobe Systems). The number of dynein arms was counted in >10 axonemes from three independent samples.

**Analysis of Cilia-Driven Flow.** Ciliary transport on the surface of intact tracheas was analyzed in transient organ culture. To visualize cilia-generated fluid flow, 10-μm-diameter polystyrene beads (Invitrogen) were loaded onto the tracheal surface. The movement of the beads was observed with a Nomarski microscope (Zeiss) equipped with a water-immersible 20× objective lens (Zeiss) and a CCD camera (Hamamatsu Photoics). The data were recorded with household digital video camera (Hitachi) for 5 min. The velocity of each bead was estimated by dividing the width of the field of view (50 μm) by the time each individual bead took to travel across the field.

**Analysis of Ciliary Beating Orientation.** Three independent samples and at least 10 fields of view in each sample were analyzed. The orientation of beating was calculated from the slope of the beating plane using Microsoft Excel. Analyses were performed as described previously (7–9).

**Histological Analysis.** Mice were perfused with 4% PFA/1% GA under anesthesia with diethyl ether. Then the heads were removed, skinned, and further fixed in Carnoy's fixative at 4 °C for 2 h. After acid decalcification (~24 h), the heads were embedded in paraffin and sectioned at ~4 μm thickness. Sections were stained with H&E or Alcian blue.

**Analysis of Coughing- or Sneezing-Like Phenotypes.** To quantify the frequency of coughing-/sneezing-like noises, animals were recor-

ded using a household digital video camera (Hitachi) for 1 min in a silent room. The recorded audio file was extracted, and a spectrogram of the recording was drawn by free software working in Windows Media Player (Microsoft). Spikes shown in the spectrogram were counted. Three animals for each genotype were analyzed. Data are given as mean ± SD.


1. Ostrowski LE, et al. (2009) Conditional deletion of *Dnaic1* in a murine model of primary ciliary dyskinesia causes chronic rhinosinusitis. *Am J Respir Cell Mol Biol* 10.1165/rcmb.2009-0118OC.
2. Wolff A, et al. (1992) Distribution of glutamylated α and β-tubulin in mouse tissues using a specific monoclonal antibody, GT335. *Eur J Cell Biol* 59:425–432.
3. Hastie AT, et al. (1986) Isolation of cilia from porcine tracheal epithelium and extraction of dynein arms. *Cell Motil Cytoskeleton* 6:25–34.
4. Penningroth SM, Cheung A, Olehnik K, Koslosky R (1982) Mechanochemical coupling in the relaxation of rigor-wave sea urchin sperm flagella. *J Cell Biol* 92:733–741.
5. Gibbons IR (1975) *Molecules and Cell Movement,* eds Inoue S, Stephens RE (Raven Press, New York), pp 207–232.
6. Dirksen ER, Zeira M (1981) Microtubule sliding in cilia of the rabbit trachea and oviduct. *Cell Motil* 1:247–260.
7. Lechtreck KF, Delmotte P, Robinson ML, Sanderson MJ, Witman GB (2008) Mutations in *Hydin* impair ciliary motility in mice. *J Cell Biol* 180:633–643.
8. Rautiainen M, Collan Y, Nuutinen J (1986) A method for measuring the orientation ("beat direction") of respiratory cilia. *Arch Otorhinolaryngol* 243:265–268.
9. De Iongh R, Rutland J (1989) Orientation of respiratory tract cilia in patients with primary ciliary dyskinesia, bronchiectasis, and in normal subjects. *J Clin Pathol* 42:613–619.
10. Fouquet JP, Prigent Y, Kann ML (1996) Comparative immunogold analysis of tubulin isoforms in the mouse sperm flagellum: Unique distribution of glutamylated tubulin. *Mol Reprod Dev* 43:358–365.
11. Gibbons BH, Gibbons IR (1974) Properties of flagellar "rigor waves" formed by abrupt removal of adenosine triphosphate from actively swimming sea urchin sperm. *J Cell Biol* 63:970–985.


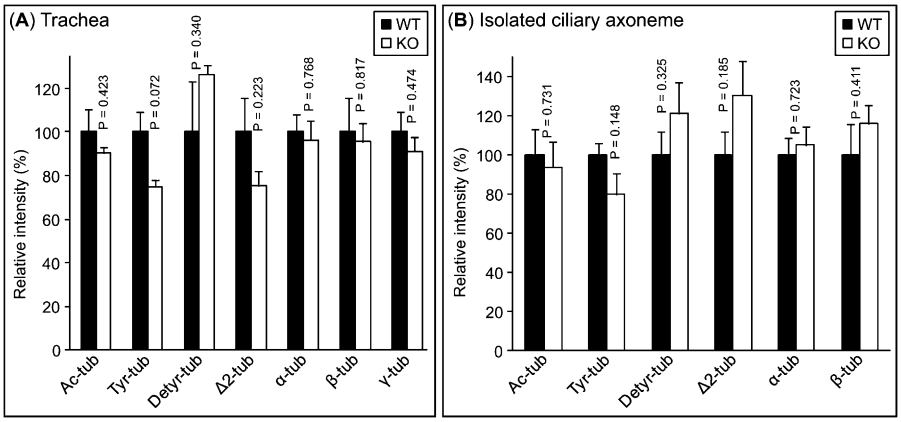


**Fig. S1.** Quantification of results of Western blot analyses. The intensity of each band was quantified by ScionImage. Data are shown as mean ± SEM (*A*, $n = 4$; *B*, $n = 5$). *P* values were analyzed by the Welch test.

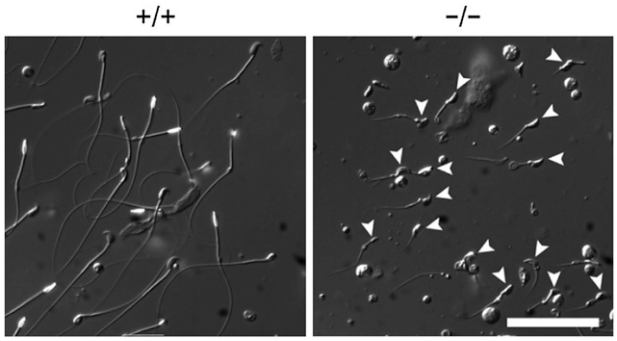


**Fig. S2.** Morphology of sperm. Sperm was obtained by dissection of the epididymis. Sperm from *Ttll1*-KO mice ($^{-/-}$) had obviously shorter flagellum (arrowheads) compared with sperm from WT mice ($^{+/+}$). (Scale bar: 50 μm.)

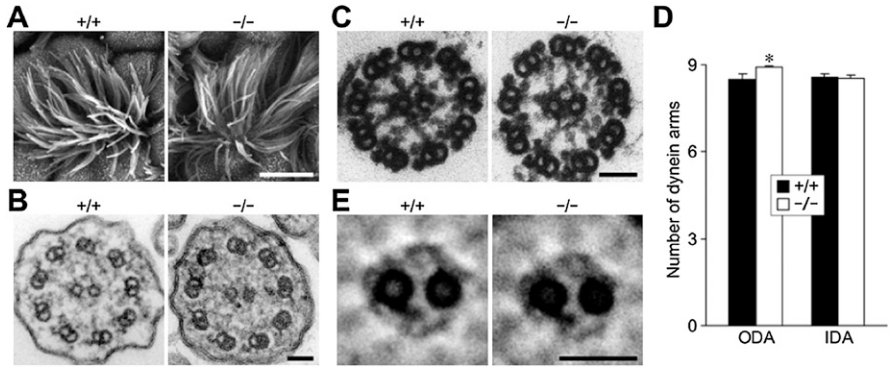


**Fig. S3.** Electron microscopy of tracheal epithelial cilia. (*A*) Representative photograph of scanning electron microscopy of tracheal epithelial cilia. Cilia were normally formed in *Ttll1*-KO ($^{-/-}$) mice. (Scale bar: 4 μm.) (*B*) Transverse views of cilia. *Ttll1*-KO ($^{-/-}$) cilium had the normal 9 + 2 structure. (Scale bar: 50 nm.) (*C*) TEM of isolated cilia axonemes. Axonemes of WT ($^{+/+}$) and *Ttll1*-KO ($^{-/-}$) tracheal cilia are shown. (Scale bar: 50 nm.) (*D*) Quantification of dynein arms. Three independent animals were examined. More than 10 axonemes were analyzed in each sample. Data are shown as mean ± SEM. Neither outer (ODA) nor inner (IDA) dynein arms were decreased in *Ttll1*-KO ($^{-/-}$) mice. (*E*) Averaged TEM of cilia axonemal central apparatus; magnified images of central doublets and central sheaths. Shown are averaged images of 32 independent photographs. There is no obvious difference between WT ($^{+/+}$) and *Ttll1*-KO ($^{-/-}$) samples. (Scale bar: 50 nm.)

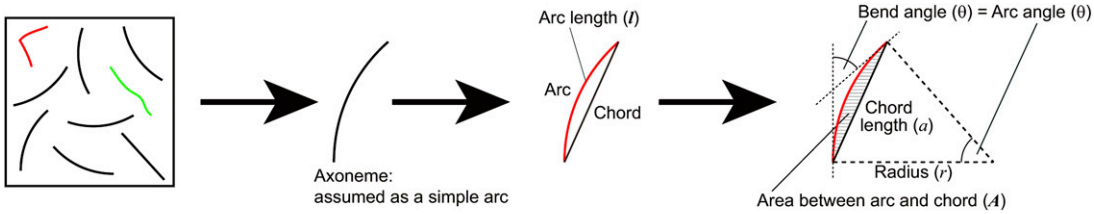


$$\begin{cases} l = r\theta \\ a = 2r\sin(\theta/2) \\ A = \dfrac{lr}{2} - \dfrac{ar\cos(\theta/2)}{2} \end{cases}$$

$$\frac{2A}{l^2}\theta^2 - \theta + \sin\theta = 0 \qquad \text{Maclaurin's expansion } (n = 0 \sim 5)$$

$$\fallingdotseq \frac{2A}{l^2}\theta^2 - \cancel{\theta} + \left\{\cancel{\theta} - \frac{\theta^3}{3!} + \frac{\theta^5}{5!} - \frac{\theta^7}{7!} + \frac{\theta^9}{9!} - \frac{\theta^{11}}{11!}\right\}$$

Thus,

$$\frac{\theta^9}{11!} - \frac{\theta^7}{9!} + \frac{\theta^5}{7!} - \frac{\theta^3}{5!} + \frac{\theta}{3!} - \frac{2A}{l^2} \fallingdotseq 0$$

This equation was solved with a tool 'Goal Seek' mounted in Microsoft Excel to obtain the arc agnle θ, which is equal to the bend angle.

Recalculation

| Given values | | Measured values | | Function | Calculation | |
|---|---|---|---|---|---|---|
| $r$ | θ (°) | $l$ | $A$ | $f(\theta)$* | θ (°) | Error |
| 10 | 5 | 0.87 | 0.01 | 0.00000 | 5 | 0.0% |
| 10 | 10 | 1.75 | 0.04 | 0.00000 | 10 | 0.0% |
| 10 | 15 | 2.62 | 0.15 | 0.00000 | 15 | 0.0% |
| 10 | 20 | 3.49 | 0.35 | 0.00000 | 20 | 0.0% |
| 10 | 30 | 5.24 | 1.18 | 0.00000 | 30 | 0.0% |
| 10 | 45 | 7.85 | 3.91 | 0.00000 | 45 | 0.0% |
| 10 | 60 | 10.47 | 9.06 | 0.00000 | 60 | 0.0% |
| 10 | 90 | 15.71 | 28.54 | 0.00000 | 90 | 0.0% |
| 10 | 120 | 20.94 | 61.42 | 0.00000 | 120 | 0.0% |
| 10 | 180 | 31.42 | 157.08 | 0.00000 | 178 | −1.2% |
| 5 | 15 | 1.31 | 0.04 | 0.00000 | 15 | 0.0% |
| 20 | 15 | 5.24 | 0.60 | 0.00000 | 15 | 0.0% |

*Function: $f(\theta) = \frac{\theta^9}{11!} - \frac{\theta^7}{9!} + \frac{\theta^5}{7!} - \frac{\theta^3}{5!} + \frac{\theta}{3!} - \frac{2A}{l^2}$

**Fig. S4.** Method of bend angle quantification. To simplify the quantification protocol, the ciliary axoneme was assumed to be a simple arc. This assumption allows easy calculation of the bend angle (θ) because the bend angle is equal to the arc angle (θ). Thus, we were able to mathematically calculate the angle (θ) by measuring two parameters, arc length (*l*) and the area between the arc and chord (*A*). The original equation was expanded with Maclaurin's expansion up to $n = 5$, and the polynomial equation was solved by the "Goal Seek" tool mounted in Microsoft Excel. The table shows the accuracy of the angle calculations. The majority of axonemes appeared as a smooth curve (black examples in the left-top box). In rare cases, small numbers of axonemes appeared to be damaged (red example) or had only a small curvature (green example). Among the rare cases, obviously damaged axonemes (red) were excluded from this assay. Axonemes that had a small curvature in a part of the axoneme (green) were analyzed by the same method, resulting in an average bend angle over the entire length of the axoneme.

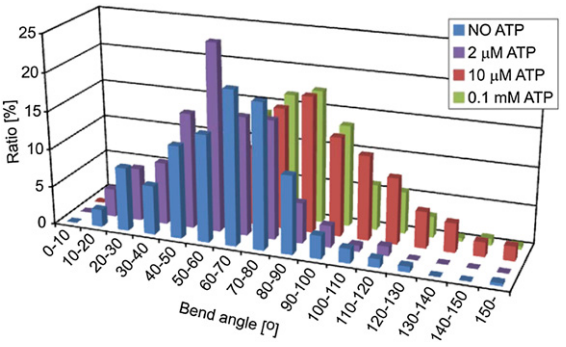


**Fig. S5.** Relaxation of ciliary axonemes by 2 μM ATP. Bend angles were decreased when ciliary axonemes were incubated with 2 μM ATP for 15 min, compared with untreated axonemes. Axonemes reactivated by 0.1 mM ATP showed larger bend angles, resulting from fixations of actively beating cilia by glutaraldehyde. *n* = 263 (no ATP), 244 (2 μM ATP), and 219 (0.1 mM ATP).

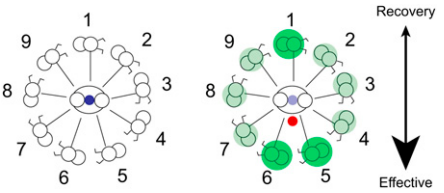


**Fig. S6.** A model of ciliary asymmetry. The structural centroid is placed in the center of the axoneme (blue circle). If tubulin polyglutamylation is distributed unevenly in cilia, as described for sperm flagella (10), then the centroid of modification moves to the side of doublets 5 and 6 (red circle), which is located in the direction of the effective stroke (11).

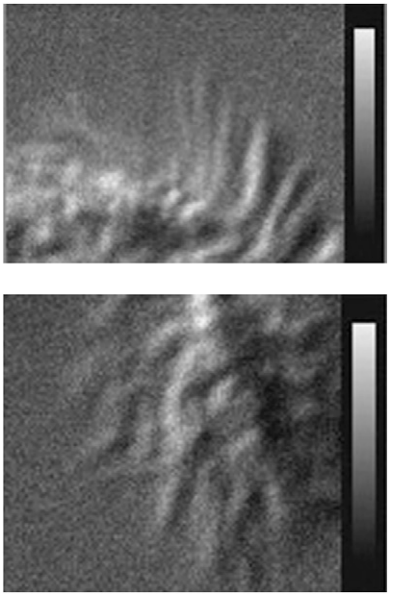

**Movie S1.** Ciliated cortices purified from WT mouse tracheal epithelia. The first half of the movie shows relaxed axonemes exposed to 5 μM ATP. The last half shows reactivated axonemes exposed to 0.1 mM ATP. Replacement of solution was done with a perfusion system.

Movie S1

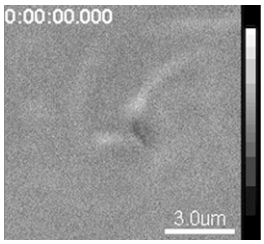


**Movie S2.** Motility of 1 mM ATP-reactivated axonemes isolated from a WT mouse. The movie is recorded at 127 fps and run at 12.7 fps (i.e., it is presented in 10-fold slow motion).

Movie S2

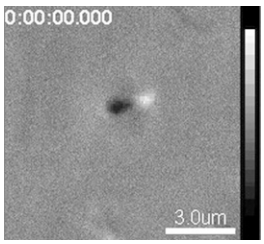


**Movie S3.** Motility of 1 mM ATP-reactivated axoneme isolated from a *Ttll1*-KO mouse. The movie is recorded at 127 fps and run at 12.7 fps (i.e., it is presented in 10-fold slow motion).

Movie S3

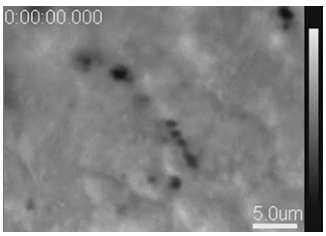


**Movie S4.** Cilia motility in transient organ culture of trachea prepared from a WT mouse. Cilia tips are labeled with Indian ink to facilitate visualization of the cilia motility. The movie is recorded at 127 fps and run at 12.7 fps (i.e., it is presented in 10-fold slow motion).

Movie S4

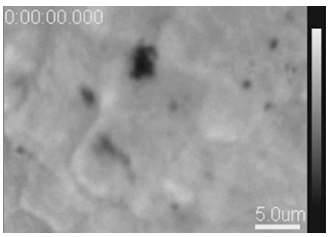


**Movie S5.** Cilia motility in transient organ culture of trachea prepared from a *Ttll1*-KO mouse. Cilia tips are labeled with Indian ink to facilitate visualization of the cilia motility. The movie is recorded at 127 fps and run at 12.7 fps (i.e., it is presented in 10-fold slow motion).

Movie S5

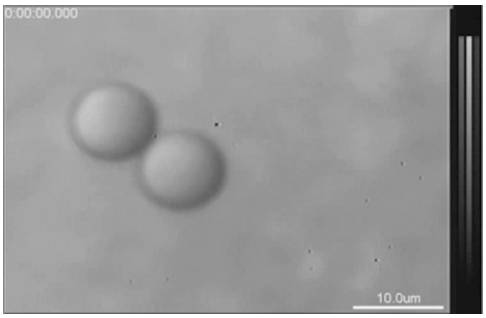


**Movie S6.** Transport of 10-μm beads over the surface of a WT trachea by normal mucociliary function. Left, the side of lung; right, the side of larynx. The movie is run at real speed. (Scale bar: 10 μm.)

Movie S6

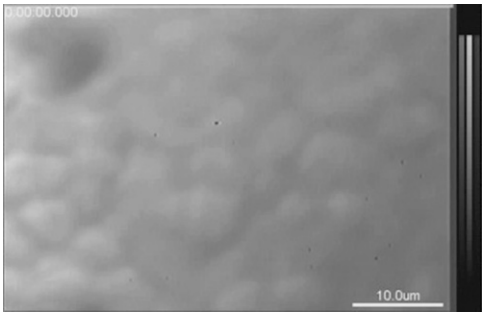


**Movie S7.** Transport of 10-μm beads over the surface of a *Ttll1*-KO trachea. Left, the side of lung; right, the side of larynx. The movie is run at real speed. (Scale bar: 10 μm.)

Movie S7

**Movie S8.** A *Ttll1*-KO mouse exhibiting coughing-like noises. (Please watch the movie with the speakers or headphones of your PC turned on.)

Movie S8

**Movie S9.** A *Ttll1*-KO mouse exhibiting both sneezing-like and coughing-like noises. (Please watch the movie with the speakers or headphones of your PC turned on.)

Movie S9

**Movie S10.** A WT mouse with no coughing- or sneezing-like noises. (Please watch the movie with the speakers or headphones of your PC turned on.)

Movie S10

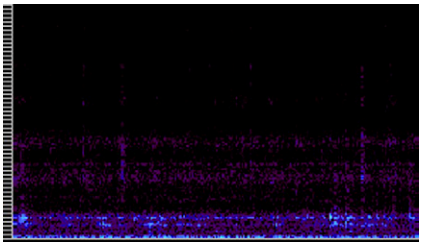

**Audio S1.** Sounds recorded from a *Dnaic1*-KO mouse, with frequent coughing-/sneezing-like noises.

Audio S1

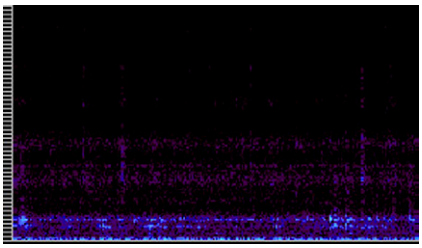

**Audio S2.** Sounds recorded from a WT mouse, with no coughing-/sneezing-like noises.

Audio S2